Available online at www.sciencedirect.com

SCIENCE DIRECT®

Materials Science and Engineering C 25 (2005) 370 – 376

MATERIALS SCIENCE & ENGINEERING C

www.elsevier.com/locate/msec

Effect of Ta content on mechanical properties of Ti–30Nb–*X*Ta–5Zr

Nobuhito Sakaguchi[a], Mitsuo Niinomi[b,*], Toshikazu Akahori[b], Junji Takeda[b], Hiroyuki Toda[b]

[a]*Toyohashi University of Technology, 1-1, Hibarigaoka, Tempaku-cho, Toyohashi 441-8580, Japan*
[b]*Toyohashi University of Technology, Department of Production Systems Engineering, 1-1, Hibarigaoka, Tempaku-cho, Toyohashi 441-8580, Japan*

Available online 12 May 2005

Abstract

In this study, we investigated the effect of Ta content on the mechanical properties of Ti–30Nb–*X*Ta–5Zr fabricated by a powder metallurgy method, for biomedical applications. The Ta content ranged from 0% to 20 mass%.

The microstructures of Ti–30Nb–*X*Ta–5Zr that contain less than 5 mass% Ta comprise β phase and an ω phase. The tensile properties of Ti–30Nb–*X*Ta–5Zr change with a change in their deformation mechanisms. The deformation mechanisms of Ti–30Nb–*X*Ta–5Zr, which contains less than 10 mass% Ta, is the stress-induced martensite (SIM) transformation, while that of Ti–30Nb–*X*Ta–5Zr, which contains over 20 mass% Ta, is the slip mechanism. The minimum elastic modulus is obtained in Ti–30Nb–10Ta–5Zr, which comprises a single β phase.

Keywords: Titanium alloy; Ta content; Deformation mechanism; Elastic modulus; Microstructure; Biomaterial; Powder metallurgy

1. Introduction

Ti–Nb–Ta–Zr system β-type alloys, such as Ti–29Nb–13Ta–4.6Zr [1–7], Ti–35Nb–7Zr–5Ta [8], and so on, which comprise non-toxic elements, have been developed for biomedical applications. In particular, Ti–29Nb–13Ta–4.6Zr, which has been developed by the authors, has been reported to possess excellent properties required for biomaterials, such as excellent tensile properties [1], excellent fatigue properties [2–4], excellent frictional wear properties [2], low elastic modulus [1,2,5], excellent remodeling of bone [5], low cytotoxicity [2], excellent bioactive ceramic coating ability [6,7], and so on. Furthermore, it was suggested that super-elastic properties appeared in Ti–29Nb–13Ta–4.6Zr [9]. An investigation needs to be conducted to clarify these super-elastic properties, tensile properties, and deformation mechanisms of Ti–Nb–Ta–Zr system alloys.

The tensile properties and deformation mechanisms of Ti–*X*Nb–10Ta–5Zr (X=0%, 10%, 15%, 20%, 25%, 30%, 35%, and 40%) based on Ti–30Nb–10Ta–5Zr, with a simplified chemical composition similar to that of Ti–29Nb–13Ta–4.6Zr, were investigated previously [9,10]. During the investigation, an elastic deformation characteristic that disobeys Hooke's law was identified in Ti–30Nb–10Ta–5Zr, and a stress-induced martensite transformation (SIM) was observed in Ti–20Nb–10Ta–5Zr and Ti–25Nb–10Ta–5Zr. Furthermore, the elongation of Ti–25Nb–10Ta–5Zr was also found to be over 40%.

However, the effect of the Ta or Zr contents on the tensile properties and the deformation mechanisms of the Ti–Nb–Ta–Zr alloy system have not been investigated. Therefore, the effect of Ta content on tensile properties and the deformation mechanisms of Ti–30Nb–*X*Ta–5Zr were investigated in this study.

2. Experimental procedures

2.1. Manufacturing process

Ti–30Nb–10Ta–5Zr (hereafter, referred to as *10Ta*), which comprises the simplified chemical composition of Ti–29Nb–13Ta–4.6Zr developed for biomedical applica-

* Corresponding author.
E-mail address: Niinomi@sp-Mac4.tutpse.tut.ac.jp (M. Niinomi).

0928-4931/$ - see front matter © 2005 Elsevier B.V. All rights reserved.
doi:10.1016/j.msec.2005.04.003

tions, was selected as a basic compositional alloy. The Ta content of this alloy was varied by four levels of 0 mass%, 5 mass%, 15 mass%, and 20 mass%. Hereafter, these alloys will be referred to as *0Ta*, *5Ta*, *15Ta*, and *20Ta*, respectively.

lThe blended elemental powder metallurgy method was used to fabricate these alloys. The mean particle sizes and purity of the powdered alloying elements used in this study were below 45 μm and over 99.8% (Ti powder: Sumitomo Sitix of Amagasaki, Inc., Japan; Nb powder: H.C. Starck GmbH and Co. KG., Germany; Ta powder: H.C. Starck-V TECH Ltd., Japan; and Zr powder: Kojundo Chemical Lab. Co., Ltd., Japan). The powder of the alloying elements was mixed to achieve each target chemical composition and then pressed to form a green product with a diameter of 40 mm and a length of approximately 100 mm, by a cold isostatic pressing machine. Each green product was then sintered at 1573 K for 57.3 ks in a vacuum of approximately 1.33×10^{-3} Pa. Subsequently, each sintered green product was forged and swaged at 1223 K to form a bar with a diameter of 10 mm. Finally, each swaged bar was subjected to heat treatment at 1123 K for 1.8 ks followed by air cooling in order to remove the residual stress resulting from hot forging and hot swaging. The chemical composition of each Ti–30Nb–*X*Ta–5Zr alloy is listed in Table 1.

2.2. Tensile tests and loading–unloading tensile tests

Dog bone-type specimens with a diameter of 3 mm and a gage length of 11 mm for tensile tests were machined from the heat-treated bars of Ti–30Nb–*X*Ta–5Zr. The geometry of the tensile test specimen is shown in Fig. 1. The machined specimens were wet-polished using waterproof emery papers up to #1500. As stated above, tensile tests were carried out on the finished specimens using an Instron-type machine (AGS-20kNG, Shimadzu Co., Japan) with a crosshead speed of 8.33×10^{-6} m/s in air at room temperature. The strain was measured using a foil strain gage attached directly to the gage section of the specimen.

Loading–unloading tensile tests were carried out using the same machine and similar specimens. During the loading–unloading tensile tests, the crosshead was stopped at strains of 1.3% and 2.0%, and the load was then released after attaining each targeted value of strain. Finally, the specimen was loaded to fracture.

Table 1
Chemical compositions of Ti–30Nb–*X*Ta–5Zr (mass%)

	0Ta	*5Ta*	*10Ta*	*15Ta*	*20Ta*
Ti	Bal.	Bal.	Bal.	Bal.	Bal.
Nb	29.7	29.8	29.4	29.8	29.9
Ta	–	4.97	10.4	15.0	20.0
Zr	4.55	4.57	4.80	4.57	4.58
O	0.22	0.23	0.23	0.25	0.25

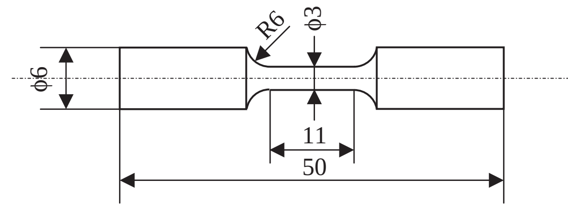

Fig. 1. Specimen geometry of dog bone-type specimen in millimeters.

Tensile tests and loading–unloading tensile tests were performed on three samples in order to determine their tensile properties.

2.3. Measurement of elastic modulus

Specimens for measuring the elastic modulus with a diameter of 6 mm and a length of 60 mm were also machined from the heat-treated bars of Ti–30Nb–*X*Ta–5Zr. These specimens were then wet-polished using waterproof emery papers up to #1500. The elastic modulus was measured using a free resonance method elastic modulus-measuring device (JE-RT, Nihon Techno-Plus Co., Ltd., Japan) in air, at room temperature. Elastic modulus measurements were performed on three samples.

2.4. Microstructural observation and identification of constituent phases

For optical microscope observation, cylindrical specimens with a diameter of 6 mm and a length of 5 mm were machined from the heat-treated bars of Ti–30Nb–*X*Ta–5Zr. Each specimen was mirror-finished by buff polishing after being polished using a #1500 waterproof emery paper. After mirror finishing, each specimen was etched in a 5% HF solution. The microstructure of each specimen was observed using an optical microscope (ECLIPSE ME600, Nikon Co., Japan).

For transmission electron microscopy (TEM) observation, disk specimens with a diameter of 2.9 mm and thickness of 0.5 mm were machined from the heat-treated bars and the vicinities of the fracture surfaces of the tensile-tested specimens of Ti–30Nb–*X*Ta–5Zr. These disk specimens were electro-polished to make thin foils. The microstructure of the thin foil was observed using a TEM (H-800, Hitachi Ltd., Japan), with an accelerating voltage of 200 kV.

In order to identify the constituent phases of Ti–30Nb–*X*Ta–5Zr, X-ray diffraction analyses (XRD) with a Cu-Kα tube were carried out using an X-ray diffractometer (RINT-2200, Rigaku Co., Japan) on the same specimens that were used for optical microscope observations. In XRD, the accelerating voltage and current were 40 kV and 30 mA, respectively.

Optical microscope observations, TEM observations, and XRD were performed on more than three samples in order to determine the microstructures and constituent phases. The